

Regular Article

Monte Carlo Calculation of Relative Dose Distribution and Dosimetry Parameters for an ¹⁹²Ir Source in a Water Phantom Using MCNP4C

A. Binesh², A.A. Mowlavi¹, and H. Arabshahi^{3*}

¹Department of Physics, Sabzevar Tarbiat Moallem University, Sabzevar, Iran; ²Department of Physics, Payam Nour University, Fariman, Iran; ³Department of Physics, Ferdowsi University of Mashhad, Mashhad, Iran

Abstract

The dose distribution has been calculated around a high dose rate ¹⁹²Ir source located in the center of 30 cm × 30 cm × 30 cm water phantom cube using MCNP code by Monte Carlo method. The percentage depth dose (PDD) variation along the different axis parallel and perpendicular the source are calculated. Then, the isodose curves for 50%, 25%, 10% and 1% PDD have been presented. The Monte Carlo results are in fair agreement with the experiment dosimetry by Gafchromic Rtqa film. Finally, dosimetry parameters of TG-43 protocol have been determined and compared with the results of others.

Keywords: Brachytherapy, Dose distribution, Monte Carlo method, MCNP code, Anisotropy function, Gafchromic Rtqa film

Introduction

Theoretical and experimental studies have been applied for dosimetric parameters determination of the brachytherapy sources¹⁻³. Usually, Monte Carlo method has been used to define such quantities as the anisotropy dose function, the radial dose function, and the dose calculation close to the source in brachytherapy⁴⁻⁶.

¹⁹²Ir source is used widely in brachytherapy to treat localized tumors near body site. Daskalov et al.⁷ have done dosimetric modeling of

the microelectron HDR ¹⁹²Ir source by the multigroup discrete ordinates method. In this present work, we have used MCNP4C⁹ code to calculate relative dose and anisotropy dose function and radial dose function TG-43 dosimetry parameters of microelectron HDR ¹⁹²Ir in a water phantom. The result is in agreement with the experiment dosimetry data which have been measured by Gafchromic Rtqa film.

The ¹⁹²Ir Source

The internal construction and dimensions of the HDR ¹⁹²Ir source is illustrated in Fig. 1. The simulated source is a cylinder of about 30% Ir and 70% Pt with 21.704 g/cm³ density, encased in a stainless steel. We assumed the radioactive material is uniformly distributed within the ¹⁹²Ir active core. The decay scheme of ¹⁹²Ir is available on-line in the Nuclear Data Base of the IAEA. The photons spectrum emitted per decay of ¹⁹²Ir and their intensity are listed in Table 1². Pia et al.⁵ used the monochromatic spectrum at 356 keV in their simulation with GEANT4 for brachytherapy treatment. Fig. 2 shows the real and monochromatic spectra. We will see that the real spectrum is important in dose calculation near and far from the source.

Fig. 1: Schematic of the ¹⁹²Ir source

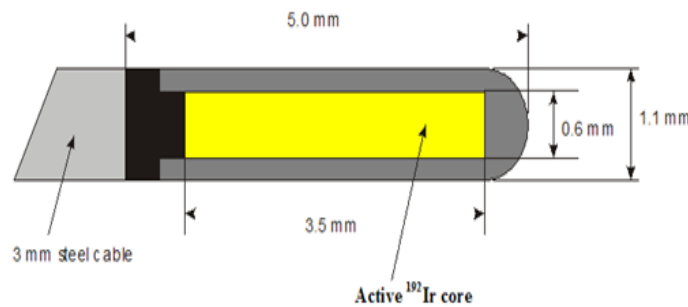
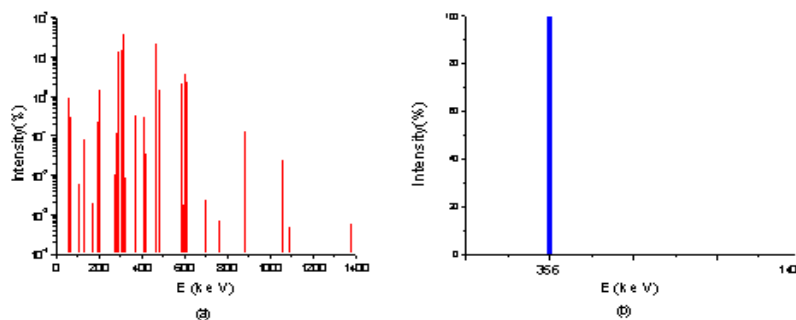


Fig. 2: (a) The real spectrum of ¹⁹²Ir and (b) the monochromatic at 356 keV



* Corresponding Author, Email: arabshahi@um.ac.ir

Table 1: Photons spectrum of ¹⁹²Ir per decay

Isotope	Energy(keV)	Intensity
Os (x-ray)	61.49	0.0016
Os (x-ray)	63	0.0203
Os (x-ray)	71.3	0.006629
Os (x-ray)	73.4	0.001732
Os	110.09	1.27E-04
Pt	136.34	0.001836
Pt	176.98	4.29E-05
Os	201.3	0.004719
Os	205.8	0.03303
Pt	280.04	2.33E-04
Os	283.27	0.002627
Pt	295.96	0.2867
Pt	308.47	0.3269
Pt	316.51	0.8286
Os	329.31	1.86E-04
Os	374.49	0.007208
Pt	416.47	0.006644
Os	420.53	7.34E-04
Pt	468.07	0.4783
Os	484.58	0.03187
Pt	485.3	2.20E-05
Os	489.04	0.004433
Pt	588.59	0.04515
Pt	593.37	4.25E-04
Pt	599.4	3.88E-05
Pt	604.42	0.08232
Pt	612.47	0.05309
Os	703.98	5.34E-05
Pt	766	1.49E-05
Pt	884.54	0.002919
Pt	1061.48	5.28E-04
Pt	1089.7	1.07E-05
Pt	1378.3	1.24E-05

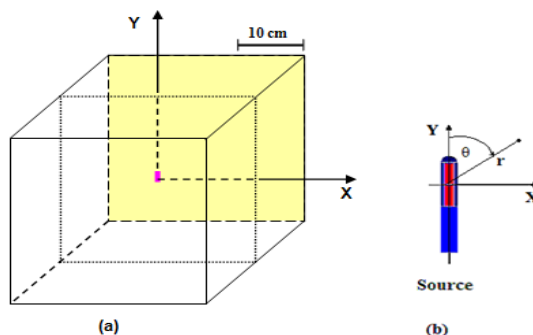
Dose calculating and measuring in water phantom

Relative dose calculation

In the present work, the dose distribution has been calculated around the ¹⁹²Ir located in the center of 30 cm × 30 cm × 30 cm water phantom cube (Fig. 3) by using tally F6:p of MCNP code. In order to use variance reduction techniques of MCNP, we used F6:p tally in our calculation. Tally F6 was evaluated in the sphere 0.1 mm diameter cell as dose in the point center of sphere. The first, along

the X axis with 0.2mm step and along the Y axis with 0.2mm step, relative dose curves have been calculated. Dose at x=1.5 mm, y=0 mm point is selected as the 100% reference point for the percentage depth dose (PDD) scale. Then, the isodose points were founded by interpolate from relative dose curves. Because of source symmetry along the Y axis, dose variation along the X axis is the same as along the Z axis; so the isodose curves in XY surface can be extended to isodose surfaces in 3-dimension XYZ space.

Fig. 3: (a) Scheme of water phantom and ¹⁹²Ir source located in the centre cube. (b) the source in large size



Dose measurement

The dose measurement has been done by using Gafchromic Rtgq film which is designed for routine quality systems management of all modalities of radiotherapy with ease and confidence in 0.02 Gy to 8 Gy dynamic ranges. PDD along x=2.5 mm and y=10 mm are compared with the Monte Carlo result in the next section.

Results and Discussions

Fig. 4 shows the PDD variation along the x=0, the effect of source shield is clear in this figure. Fig. 5-a shows the Monte Carlo and experimental PDD along x=2.5 mm which are in good agreement, also in Fig. 5-b the both result are shown along y=10 mm, in $x \in [-25 \text{ mm}, 25 \text{ mm}]$ interval the results are well match but out of this range the Monte Carlo result is lower estimated. The isodose curves for 50%, 10%, 3%, and 1% and a typical PLATO result are showed at Fig. 6. PLATO Brachytherapy software module provides image based planning and 3D visualization as a standard feature. In 1995, the Cleveland Clinic Foundation Taussig Cancer Centre initiated a Nucletron Microselectron ¹⁹²Ir remote after loading system into the Brachytherapy Service (Microselectron/Plato Planning System). This system utilizes the Plato Dosimetry Planning Software, which allows source dwell-time optimization to minimize heterogeneity of dose distribution, a notable advance in the field of interstitial brachytherapy. It can be seen easily $D = D(r, \theta)$, dose distribution depends to r and θ , distance from the center of the source and polar angle, respectively. The results can be used for computation of model dependent parameters like anisotropy dose function. As it mentioned before, Pia et al. ⁵ used the monochromatic spectrum at 356 keV in their simulation; because of energy dependency of attenuation coefficient, dose deposit of monochromatic and real spectrum source is different close and far from the source. Fig. 7 shows the dose variation and relative deflection dose along the y=0 for both spectra. Far from the source, deflection dose reach to 13% and near the source it is 5% which due to the absorbing of low energy photons near the source and reaching some high energy photons to far distance of the source.

Anisotropy function is an important parameter than we can compare our result with which was obtained by others. According to TG-43 protocol (Nath et al., 1995), the absorbed dose can be expressed as:

$$D(r, \theta) = S_k \Lambda t \frac{G(r, \theta)}{G(r_0, \theta_0)} g(r) F(r, \theta) \quad (1)$$

where S_k is the air kerma strength, Λ is the dose rate constant, $G(r, \theta)$ is the geometry factor, $F(r, \theta)$ is the anisotropy function, $g(r)$ is radial dose function, and (r_0, θ_0) is the reference point. So, the anisotropy function can be expressed by following equation:

$$F(r, \theta) = \frac{D(r, \theta)}{D(r_0, \theta_0)} \frac{G(r_0, \theta_0)}{G(r, \theta)} \quad (2)$$

Fig. 8 shows a comparison of $F(5 \text{ cm}, \theta)$ obtained with experimental and Monte Carlo methods by Ancil et al. ¹¹, Baltas et al. ¹², Williamson et al. ¹³ and our results. It can be seen a good agreement between this work and experimental/Monte Carlo results of the others.

Fig. 4: PDD variation along the x=0 mm

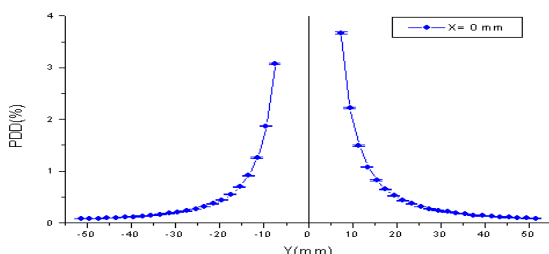


Fig. 5: The Monte Carlo and experimental PDD: (a) along x=2.5 mm and (b) along y=10 mm

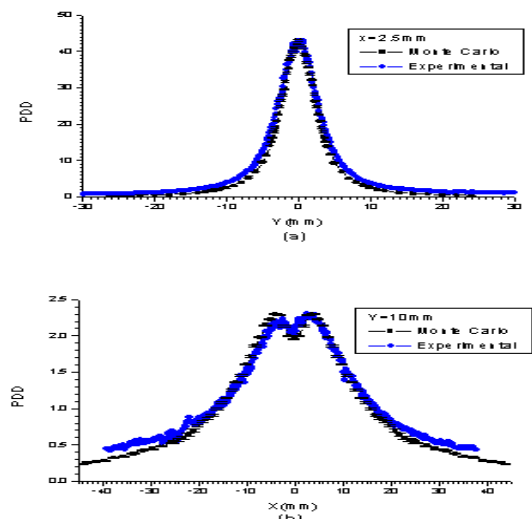


Fig. 6: (a) The isodose curves calculated by MCNP (the reference Point: x=1.5mm, y=0mm) (b) A typical isodose curves of PLATO

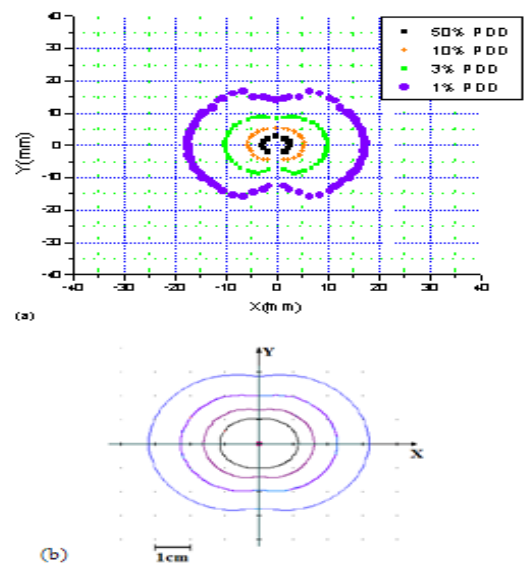


Fig. 7: (a) The dose variation and (b) relative deflection dose along the y=0

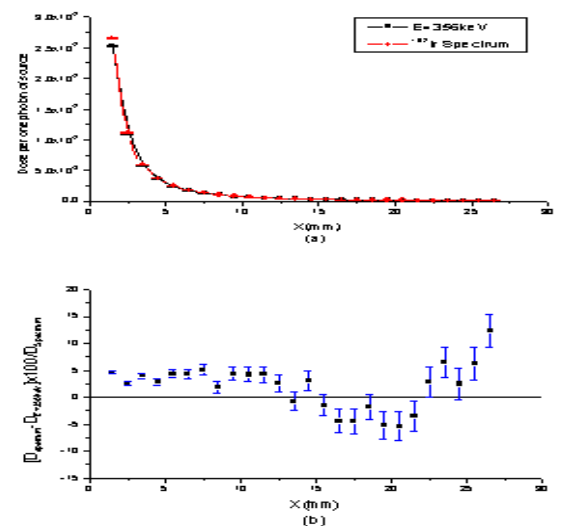


Fig. 8: Comparison of $F(5 \text{ cm}, \theta)$ obtained with experimental (Exp.) and Monte Carlo (MC) methods by others

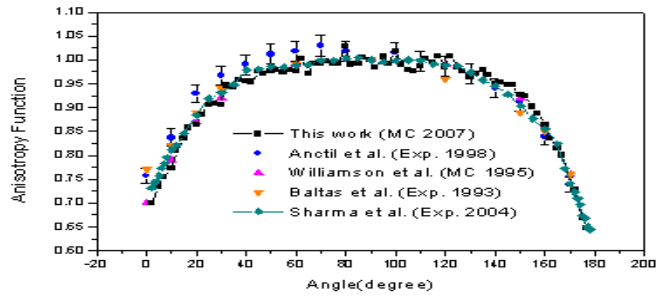


Table 2: $F(r, \theta)$

θ (deg)	$F(1, \theta)$	$F(2, \theta)$	$F(3, \theta)$	$F(4, \theta)$	$F(5, \theta)$	$F(6, \theta)$
2	0.64241	0.63915	0.65992	0.68651	0.69887	0.72382
5	0.66621	0.66642	0.69096	0.71967	0.73461	0.74318
7	0.6937	0.69556	0.71123	0.73836	0.75377	0.76434
10	0.73364	0.7301	0.75023	0.76241	0.77316	0.7954
12	0.76024	0.75458	0.77558	0.80236	0.80978	0.81983
15	0.7916	0.79302	0.81355	0.83165	0.83591	0.83217
17	0.81585	0.80937	0.81771	0.84667	0.85742	0.85416
20	0.84203	0.8292	0.85143	0.86094	0.865	0.87222
22	0.86264	0.84939	0.86392	0.89347	0.88544	0.90458
25	0.88336	0.87149	0.88065	0.90299	0.90687	0.91422
27	0.8951	0.87861	0.88308	0.891	0.90798	0.89614
30	0.90793	0.88533	0.91049	0.9296	0.90656	0.92017
32	0.92073	0.9089	0.9247	0.93725	0.94609	0.95147
35	0.92826	0.92669	0.91972	0.94445	0.94311	0.94597
37	0.93584	0.91915	0.92737	0.95518	0.95789	0.95024
40	0.95042	0.93698	0.93541	0.96729	0.95467	0.95361
42	0.95613	0.94149	0.94195	0.95692	0.95405	0.97385
45	0.96505	0.94425	0.94477	0.96914	0.97556	0.98146
47	0.96741	0.94734	0.96933	0.97479	0.97127	0.9731
50	0.97446	0.96079	0.95799	0.97101	0.97597	0.95426
52	0.97207	0.95598	0.9787	0.98953	0.97954	0.98609
55	0.98516	0.95989	0.97482	0.97569	0.9734	0.99102
57	0.98586	0.96797	0.97576	0.97817	0.9792	1.00015
60	0.98143	0.96691	0.97693	0.98374	0.97601	0.97314
62	0.98748	0.96833	0.98246	0.98945	1.00337	1.00622
65	0.98986	0.97383	0.98639	0.98956	0.972	0.97463
67	0.99222	0.97739	0.98369	0.99928	0.99147	1.00321
70	0.99471	0.98045	0.99498	0.99247	0.9927	0.99232
72	0.99639	0.98186	0.97686	0.99038	0.9982	0.9728
75	0.9946	0.97582	0.96597	0.98732	0.99287	0.99863
77	0.99848	0.97192	0.98922	1.00042	0.99353	0.99211
80	0.99736	0.98212	0.99163	1.01748	1.02834	1.00412
82	0.99879	0.98066	0.99053	1.00017	0.9907	0.99095
85	1.00559	0.97788	0.98468	0.99142	0.9928	1.00232
87	1.00292	0.98301	0.99117	0.99752	1.0056	0.99227
90	1	1	1	1	1	1
92	1.00067	0.98692	0.98212	1.00023	0.98467	0.97674
95	1.00108	0.98517	0.993	0.9863	1.00671	0.98428
97	1.00047	0.97478	0.98798	0.99445	0.99221	1.02148
100	1.00153	0.98139	0.97692	0.99461	1.01848	1.0173
102	0.99855	0.98812	0.99525	0.98096	0.99085	0.99047
105	0.99962	0.98004	0.98874	0.98185	0.97897	0.98407
107	0.99879	0.98615	0.98616	0.99839	0.97546	0.9824
110	0.99049	0.97339	0.99219	1.00877	0.98654	0.99373
112	0.99596	0.97552	0.98238	1.00332	1.00341	1.01277
115	0.99437	0.98417	0.98743	1.00046	0.99522	0.99602
117	0.99234	0.97463	0.96729	0.98809	1.00715	0.98827
120	0.98826	0.97156	0.95857	0.97535	0.98535	0.98464
122	0.98429	0.96521	0.97417	0.98825	1.00833	0.99295
125	0.98016	0.96554	0.97704	0.99331	0.9846	0.98146
127	0.9762	0.95994	0.95444	0.98322	0.97622	0.98159
130	0.97458	0.952	0.95516	0.97315	0.96448	0.95998
132	0.97186	0.94859	0.94692	0.96671	0.97035	0.9743
135	0.96612	0.94958	0.94163	0.98213	0.97814	0.95433
137	0.95475	0.94341	0.93883	0.9658	0.96903	0.969
140	0.95114	0.93149	0.93711	0.95569	0.94887	0.97228
142	0.94366	0.93484	0.93319	0.96156	0.95222	0.92479
145	0.93432	0.92132	0.93152	0.94296	0.94709	0.94669
147	0.9217	0.90346	0.92276	0.94756	0.94702	0.95096
150	0.9118	0.89715	0.91158	0.91551	0.92718	0.92481
152	0.90273	0.88853	0.86716	0.92236	0.92459	0.91976
155	0.87201	0.87026	0.84913	0.89974	0.90206	0.90922
157	0.86667	0.85394	0.84338	0.88873	0.88769	0.90511
160	0.84337	0.8354	0.84036	0.85617	0.86429	0.85057
162	0.81845	0.8095	0.76537	0.83383	0.83511	0.84584
165	0.77729	0.76828	0.75506	0.80021	0.8138	0.82221
167	0.75044	0.74017	0.71774	0.79248	0.80014	0.79095
170	0.68847	0.68176	0.70189	0.7306	0.73805	0.75946
172	0.63953	0.64537	0.59018	0.70204	0.72751	0.73444
175	0.57043	0.58387	0.58231	0.65603	0.6679	0.68588
177	0.54585	0.56259	0.57612	0.61418	0.64652	0.6532

Conclusions

Monte Carlo simulation in brachytherapy is useful to obtain model dependent parameters and to verify PLATO data, since the computational result is more accurate than the analytical PLATO data. Also the results can be used for computing anisotropy dose function. Near the source, dose can be calculated accurately by Monte Carlo method because of high gradient dose variation in this region.

The present work demonstrates a useful approach using MCNP code in dose calculation that can be applied in many other fields.

References

1. Piermattei, A. Fidanzio, L. Azario, A. Rossu, F. Perrone, M. P. Toni, R. Capote, "Experimental and Monte Carlo endovascular dosimetry of a ^{192}Ir source," *Physica Medica* XIX(2), 111- 118 (2003).
2. F. Ballester, C. Hernández, J. Pe'rez-Calatayud, F. Lliso, "Monte Carlo calculation of dose rate distributions around ^{192}Ir wires," *Med. Phys.* 24(8), 1221-1228 (1997).
3. S. Kirov, J. F. Williamson, A. S. Meigooni, Y. Zhu, "Measurement and calculation of heterogeneity correction factors for an Ir-192 high dose-rate brachytherapy source behind tungsten alloy and steel shields," *Med. Phys.* 23(6), 911-919 (1996).
4. F. Foppiano, S. Agostinelli, S. Garelli, G. Paoli, M. Bevegna, M. G. Pia, P. Franzone, T. Scolaro, L. Andreucci, "Comparison between PLATO isodose distribution of a ^{192}Ir source and those simulation with GEANT4 toolkit," National Cancer Institute and Phys. Dept. of Geneva (2001).
5. M. G. Pia, F. Foppiano, S. Agostinelli, S. Garelli, G. Paoli, P. Nieminen, "The application of GEANT4 simulation code for brachytherapy treatment," 9th International Conference on Calorimetry in High Energy Physics, Annecy, 1-15 (2001).
6. Angelopoulos, P. Baras, L. Sakelliou, P. Karaikos, P. Sandilos, "Monte Carlo dosimetry of a new ^{192}Ir high dose rate brachytherapy source," *Med. Phys.* 27(11), 2521-2527 (2000).
7. G. M. Daskalov, R. S. Baker, D. W. O. Rogers, J. F. Williamson, "Dosimetric modeling of the microselectron high dose rate ^{192}Ir source by the multigroup discrete ordinates method," *Med. Phys.* 27(10), 2307-2319 (2000).
8. S. Sureka, P. Aruna, S. Ganesan, C. S. Sunny, K. V. Subbaiah, "Computation of relative dose distribution and effective transmission around a shielded vaginal cylinder with ^{192}Ir HDR source using MCNP4B," *Med. Phys.* 33(6), 1552-1561 (2006).
9. J. F. Briesmeister (editor), "MCNPTM- A general Monte Carlo N-particle transport code, Version 4C" , Los Alamos National laboratory Report LA-13709-M, (2000)
10. R. Nath, L. L. Anderson, G. Luxton, K. A. Weaver, J. F. Williamson, A. S. Meigooni, "Dosimetry of interstitial brachytherapy sources: Recommendations of the AAPM Radiation Therapy Committee Task Group No. 43," *Med. Phys.* 22, 209-234 (1995).
11. J. C. Ancil, B. G. Clark, C. J. Arsenault, "Experimental determination of dosimetry functions of Ir-192 sources," *Med. Phys.* 25(12), 2279-2287 (1998).
12. Baltas, R. Kramer, E. Löffler, "Measurements of the anisotropy of the new Ir-192 source for the microSelectron-HDR," *Activity Special Report* 3, 2 (1993).
13. J. F. Williamson, Z. Li, "Monte Carlo aided dosimetry of the microselectron pulsed and high dose-rate Ir-192 sources," *Med. Phys.* 22, 809-820 (1995).

Please Cite This Article As:

A. Binesh, A.A. Mowlavi, and H. Arabshahi. 2010. Monte Carlo Calculation of Relative Dose Distribution and Dosimetry Parameters for an ^{192}Ir Source in a Water Phantom Using MCNP4C. *J. Exp. Sci.* 1(4):32-36.